Proc. of the 8th International Symposium on Geotechnical Safety and Risk (ISGSR)
Edited by Jinsong Huang, D.V. Griffiths, Shui-Hua Jiang, Anna Giacomini and Richard Kelly
©2022 ISGSR Organizers. *Published by* Research Publishing, Singapore.
doi: 10.3850/978-981-18-5182-7_16-006-cd

Fragility Curves for Analysis of Levees Subject to Concentrated Leak Erosion

Jonathan Simm[1], Mohamed Hassan[1] and Ben Gouldby[1]

[1]HR Wallingford, Howbery Park, Wallingford OX12 8JT, United Kingdom.
E-mail: j.simm@hrwallingford.com

Abstract: This paper discusses the use of fragility curves as a way of expressing the likely performance or reliability of a levee, as part of a flood risk systems analysis and/or to support asset specific decision-making. In terms of geotechnical mechanisms, the focus of the paper is on concentrated leak erosion, the form of internal erosion believed to be most relevant to UK levees. The paper discusses the use of fragility curves combined with asset-specific extreme loading distributions to determine a national database of asset annual failure probabilities as a one means of prioritizing future detailed inspections, investigations and interventions.

Keywords: Fragility curve; flood risk; under-seepage piping; concentrated leak erosion; prioritization.

1 Representing internal erosion in fragility curves.

Internal erosion involves the detachment of soil particles and their transport by seepage flow. It can involve one or more of four principal internal erosion mechanisms (CIRIA, 2013):

(a) Contact erosion: related to selective erosion of fine particles from the contact with a coarser layer;

(b) Backwards erosion: occurring along a decompressed contact area as a result of seepage exiting an unfiltered surface; it leads to retrogressively growing soil piping and sand boils and is typically linked to permeable layers lying beneath a surficial less permeable ground surface on which a levee may be situated;

(c) Concentrated leak erosion: related to the detachment of soil particles through a pre-existing path, such as a crack. Given the through-levee silt or clay composition of most UK flood embankments, this mechanism is believed to be the most important transverse internal erosion process for transitions between soil and hard structures;

(d) Suffusion: related to the selective erosion of the fine particles from a matrix of coarse particles.

In England the most commonly occurring mechanisms are (b) and (c). Backwards erosion ('piping') is limited to a few situations such as the Thames estuary where under-seepage through permeable layers can occur. Concentrated leak erosion is believed to be the more common mechanism, typically linked to animal burrowing within the levee, to geotechnical discontinuities in the levee (including those generated by pipes and culverts) and to transitions from levees to flood walls

The process of internal erosion can broadly be broken into four phases: initiation, continuation, progression to form an erosion piping zone (causing surface sloughing) and initiation of a breach (Morris *et al*, 2012). For risk analysis purposes, the initiation phase is taken to be the critical issue to determine, although for subsequent inundation assessments breach widths and breach hydrographs are also required. The initiation phase is described using fragility curves to represent the probability of occurrence of a particular internal erosion mechanism conditional on loading.

Representation of the two selected mechanisms follows approaches already established in the literature.

(a) backward erosion piping arising from under seepage. This mechanism is represented using the classical approaches summarized in ICOLD (2016). The process of backward erosion can only take place if there is prior heave of any surface impermeable layer landward of the levee, allowing piping to progress at the interface of the underlying permeable layer with this upper layer. This means that that the calculated probability of backward erosion piping commencing must be multiplied by (reduced by) the probability of the heave of the surface impermeable layer, if it is present.

(b) concentrated leak erosion. There is much less discussion of this mechanism in the literature, although ICOLD (2016) Bulletin 164 sets out the processes unambiguously. For this reason we discuss this mechanism in detail in the following sub-section, explaining how we assess the various governing parameters

1.1 Concentrated leak erosion

The process involves initial erosion along the walls of the crack (ICOLD, 2016) and continuation of this erosion leading to enlargement of the crack eventually resulting in breach.

ICOLD (2016) gives the following equations to determine hydraulic shear stress, depending on the crack shape. (Note that the hydraulic shear stress for a cylindrical crack is about half that for a vertical transverse crack.)

a. For cylindrical pipes:

$$\tau = \rho_w \frac{gH_f D}{4L} \tag{1}$$

b. For vertical, transverse cracks:

$$\tau = \frac{\rho_w g {H_f}^2 W}{2(H_f + W)L} \tag{2}$$

where:

ρ_w = Density of water in kg/m^3
g = Acceleration due to gravity = 9.8 m/s^2
H_f = Head loss in pipe or crack due to friction in meters
L = Length of pipe or crack base in meters
D = Diameter of the cylindrical crack in meters
W = Width of vertical crack in meters.

The shape of cracks in the body of earthen embankments generally could be cylindrical or vertical, Vertical surface cracks to a depth of 1.2 m together with some horizontal cracking were found by Dyer *et al* (2009). Cylindrical cracks may be more appropriate when considering the impact of animal burrows or decayed tree roots. In the case of transitions, the hydraulic separation that may well occur at the interface between the earthen embankment and the hard structure, means that vertical cracks between the flood embankment material and the hard structure are likely and may extend across the full width of the earthen embankment.

In terms of crack width: ICOLD (2016) recommends assuming widths of between 1 and 2 mm. In our analysis, we therefore assumed a triangular distribution of crack width between 1 and 2mm.

In terms of crack length: the longer the length of the crack the smaller the shear stress (and hence the better the reliability). For earthen embankments (including transitions) in good condition (i.e. without holes or large separations, the cracks will need to penetrate right through the structure and thus for resistance to concentrated leak erosion, the wider the structure the better. Embankments in poorer condition with defects such as animal burrows, can be represented by a reduced crack length. For our work, we assume the adjustment factors to good-condition crack lengths given in Table 1.

Table 1. Crack length adjustments based on embankment condition grade

Environment Agency visual condition grade	Description of condition grade	Factor applied to assumed crack length
1	Very Good (Cosmetic defects that will have no effect on performance)	1
2	Good (Minor defects that will not reduce the overall performance of the asset)	1
3	Fair (Defects that could reduce performance of the asset)	0.9
4	Poor (Defects that would significantly reduce the performance of the asset.)	0.5
5	Very Poor (Severe defects resulting in complete performance failure)	0.1

Head loss across the crack: the head loss across the crack length is taken to be the difference in water level between the river side (level variable) and the landward side (assumed to be either the downstream structure toe level or the ground level).

1.2 Computation of Critical Shear Stress

The approach adopted for determining critical shear stress assumed that UK soils in earthen flood embankments are non-dispersive. (Dispersive soils (see e.g. ICOLD, 2016 and Terzaghi *et al*., 1996) are structurally unstable and more erodible, sometimes significantly more so; this is because the soil aggregates – small clods – collapse when the soil gets wet because the individual clay particles disperse into solution.) Reported instances of the presence of dispersive soils in the UK are rare, but this may be because the phenomenon is poorly understood.

For non-dispersive soils, ICOLD (2016) provides the Representative Erosion Rate Indices given in Table 2, which in turn represent the relative soil erosion rates given in Table 3. ICOLD (2016) then suggests associated critical shear stress values. Given that the analysis behind fragility curves is probabilistic, we adopt a triangular distribution of assumed critical shear stress values in the analysis to get a fair representation of the uncertainties associated with allocating a particular value to a specific soil. The assumed limits and best values for the distributions are provided in Table 4.

Table 2. Representative Erosion Rate Index for Non-Dispersive Soils (ICOLD, 2016)

Unified soil classification	Representative erosion rate index (I_{HET})		
	Likely minimum	Best estimate	Likely maximum
SM with <30% fines	1	<2	2.5
SM with >30% fines	<2	2 to 3	3.5
SC with <30% fines	<2	2 to 3	3.5
SC with >30% fines	2	3	4
ML	2	2 to 3	3
CL-ML	2	3	4
CL	3	3 to 4	4.5
CL-CH	3	4	5
MH	3	3 to 4	4.5
CH with liquid limit <65%	3	4	5
CH with liquid limit <65%	4	5	6

Where: SM = Silty sand; SC = Clayey sand; ML = Silt; MH = Silt of high plasticity, elastic silt; CL = Clay of low plasticity, lean clay; CH = Clay of high plasticity, fat clay; and the representative erosion rate index, I_{HET}, is an index derived from the Hole Erosion Test (HET) described in ICOLD (2016)

Table 3. Soil erosion rates related to Representative Erosion Rate (IHET) Indices (ICOLD, 2016)

Representative erosion rate index (I_{HET})	Relative Soil Erosion Rate
< 2	Extremely rapid
2 – 3	Very rapid
3 – 4	Moderately rapid
4 – 5	Moderately slow
5 – 6	Very slow
> 6	Extremely slow

Table 4. Limits and best estimates for a triangular distribution of critical shear stress for different soil types

I_{HET}	Critical shear stress (Pa) limits – assuming a triangular distribution		
	Low	Best	High
Up to 3	1	2	5
3.5	2	5	25
4	5	25	60
5	25	60	100

2 Development and use of fragility curves

As explained in previous papers, an analytical approach (see e.g. Simm *et al*, 2008) has been adopted in the UK for the determination of fragility curves in the form given in Figure 1

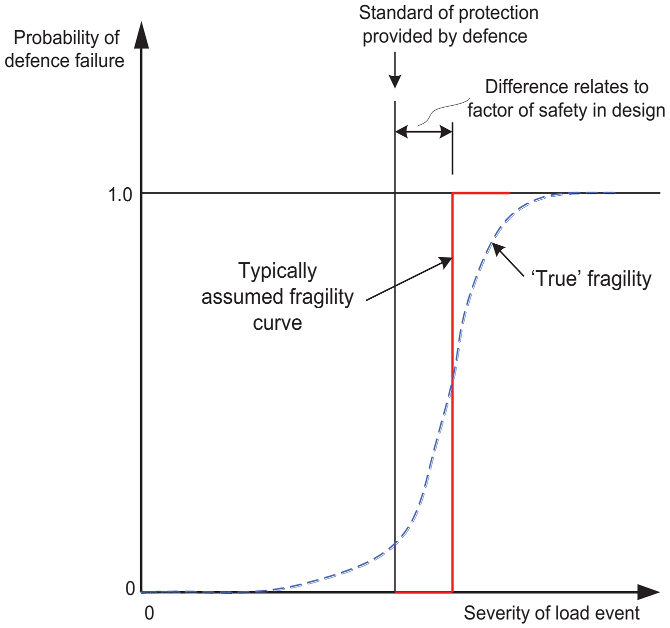

Figure 1. Conceptual diagram of a fragility curve.

To generate the fragility curve for concentrated leak erosion, the process adopted is:

1. Set up the Limit State Equation (LSE) in reliability form:

$$Z\ (\text{“reliability"}) = \tau_{crit} - \tau \qquad (3)$$

where τ and τ_{crit} are determined as described above in sections 2.1 and 2.2 respectively.

2. Produce a schedule of the engineering parameters feeding into the LSE, including defining the width and form of the uncertainty bands around each parameter. In this case the relevant parameters are those in the characterization of τ given in equations (1) and (2)

3. Perform a series of reliability analyses under each of a series of different hydraulic loading conditions (water levels for riverine levees). For any given loading condition, the analysis comprises of a series of Monte Carlo simulations, sampling from the uncertainty bands for each input parameter from the characterization of τ given in equations (1) and (2). Failure arises in a particular case when the combinations of parameter values in the limit state function Z give a value for Z which is less than or equal to zero. The probability of failure for that loading is then the number of times when the simulation gives Z as less than or equal to zero divided by the total number of simulations.

Using an appropriate fault tree, such curves can be combined with curves for other independent failure mechanisms by means of de Morgan's law

As also explained previously (Simm & Tarrant, 2018), a national dataset of generalized fragility curves is typically used in the UK for broad scale regional or national analyses such as the National Flood Risk Assessment (NaFRA). These curves are based on levee geometries and geotechnical parameters typical to the UK. Generic curves for concentrated leak erosion (and other mechanisms) are created for each of the 5 visual condition grades described in Table 1 above

Fragility curves are also used at the level of an individual levee or levee system to explore the risk associated with the deterioration of an asset below its target condition. The approach also helps the asset manager set out the cost and benefits in order to develop a case for investment. At this detailed level, the limitations of using generic fragility curves become obvious and hence HR Wallingford has developed a web-based tool (HR-RELIABLE) to permit asset managers easily to create levee specific fragility curves.

From the foregoing it will be apparent that the national/regional approach applied in the UK, developed in 2006-2007, is based on the simplifying assumption that when the interrogation of the fragility curve in the analysis indicates failure, this is assumed to be an instantaneous full failure and related fully developed breach. This is a conservative assumption because clearly in practice full failure (breach) can only occur when the subsequent breach process initiated by the internal erosion is complete; such a breach takes some time to evolve. The reason for adopting the conservative approach in the first instance was governed by computational time when we were carrying out flood risk analyses for the whole of England. However, HR Wallingford has experimented with more complex analyses as described in Gouldby et al (2014). In these studies the fragility curve was adapted to simulate the probability of breach initiation with breach growth using simple rules in a time varying model (breach growth was not the main focus of the work). Vorogushyn et al (2011) adopted a different approach of simulating breach development times stochastically. In the future, it is envisaged improved approaches will be developed, that both include dynamic breaching within flood risk systems models but are also sufficiently computationally efficient to allow large systems to be analyzed given modern computational resources.

3 Prioritizing defense management activities using annual failure probabilities

As part of a research project on the role of transitions between earthen levees and hard structures such as flood walls (Simm *et al,* 2021), a sensitivity testing exercise was undertaken looking at the impact of a range of levees and hydraulic loading characteristics on the levee fragility under the Concentrated Leak Erosion mechanism (and also under the Grass Erosion (external erosion) mechanism).. The objectives of the testing were to explore the sensitivity of the annual failure probability to a number of parameters (e.g. geometry, soils) using hydraulic loading conditions relevant to the individual levee. It was envisaged that the outcomes of the sensitivity testing would potentially support both:

a. screening out situations unlikely to pose a risk to the performance of the levee;
b. inspection/data collection by highlighting key information/defects to be prioritized for collection

The following procedure was adopted:

i. Generate the fragility curve relevant to each levee;

ii. Calculate for each fragility curve a single number, the annual failure probability by integrating the fragility curve with the distribution of extreme loadings at the site in question. This number is determined from the following relationship:

Annual p(F) = sum of (p(F) given load from fragility curve x load probability) across all loads (4)

The sensitivity analysis showed that for English earthen flood embankments, the focus of concern with regard to concentrated leak erosion should be on embankments with the following characteristics:

- heights greater than or equal to 2 meters;
- side slopes of 1:3 or steeper;
- crest widths of 4m or less (i.e. ‘narrow’ embankments, rather than ‘wide’ embankments).

4 Conclusions

This paper has discussed the development and use of fragility curves to represent concentrated leak erosion, the form of internal erosion believed to be most relevant to UK levees. The resulting curves are relevant for both large scale regional or national analyses of flood risk, but also for decision making on the management of individual levees. A sensitivity analysis has used these fragility curves combined with asset-specific extreme loading distributions to determine a national database of levee annual failure probabilities. The databases suggests that for UK levees the focus of attention on managing concentrated leak erosion should be on embankments with heights greater than or equal to 2 meters, side slopes of 1:3 or steeper and crest widths of 4m or less.

References

CIRIA (2013) International Levee Handbook (RP. Report C731. *London: CIRIA*

ICOLD, 2016. Bulletin 164: Internal erosion of existing dams, levees and dikes, and their foundations. *Paris; ICOLD*

Gouldby, B., Lhomme, J., Jamieson, S., Hornby, D. and Laeger, S. (2014) A flood risk analysis model with topographical inundation and life-loss. *Proc. Instn. Civ. Engrs. - Water Mgt*. 168-WM3: 116-128

Morris, M., Hassan, M. and van Damme, M. (2012) Recent Improvements in Predicting Breach through Flood Embankments and Embankment Dams. *In: Dams: Engineering in a Social & Environmental Context*. London: Thomas Telford

Simm, J., Gouldby, B, Sayers, P., Flikweert, J, Wersching, S and Bramley, M. (2008) Representing fragility of flood and coastal defences: getting into the detail. Proc. Eur, Conf. on Flood Risk Management: Research into Practice (FLOODrisk 2008). *London: Taylor & Francis*, 621-631.

Simm, J. and Tarrant, O. (2018) ‘Development of fragility curves to describe the performance of UK levee systems.’ *Proc. 26th Congress International Commission on Large Dams, Vienna, Austria*.

Simm, J. Hassan, M. and Woods Ballard, B. (2021). Assessing and managing risks with transitions in flood defense infrastructure: Transitions Reliability Report. *Unpublished research report for UK Environment Agency*.

Terzaghi, K., Peck, R. B. and Mesri, G. (1996) Soil Mechanics in Engineering Practice, 3rd Edition, *New York: Wiley Interscience*

Vorogushyn, S., Apel, H. and Merz, B. (2011) The impact of the uncertainty of dike breach development time on flood hazard. *Physics and Chemistry of the Earth, Parts A/B/C*, 36: 319-323